

# Environmental Conditions as Determinants of Kidney Stone Formation

Carmen González-Enguita, Gonzalo Bueno-Serrano, Andrés López de Alda-González, and Rosario García-Giménez\*



Cite This: *ACS Appl. Bio Mater.* 2023, 6, 5030–5036



Read Online

ACCESS |



Metrics & More



Article Recommendations

**ABSTRACT:** Urolithiasis is a disease characterized by the presence of stones in the urinary tract, whether in the kidneys, ureters, or bladder. Its origin is multiple, and causes can be cited as hereditary, environmental, dietary, anatomical, metabolic, or infectious factors. A kidney stone is a biomaterial that originates inside the urinary tract, following the principles of crystalline growth, and in most cases, it cannot be eliminated naturally. In this work, 40 calculi from the Don Benito, Badajoz University Hospital are studied and compared with those collected in Madrid to establish differences between both populations with the same pathology and located in very different geographical areas. Analysis by cathodoluminescence offers information on the low crystallinity of the phases and their hydration states, as well as the importance of the bonds with the Ca cation in all of the structures, which, in turn, is related to environmental and social factors of different population groups such as a high intake of proteins, medications, bacterial factors, or possible contamination with greenhouse gases, among other factors.

**KEYWORDS:** kidney stone, oxalate, struvite, rural/urban area, Don Benito (Badajoz), Madrid, Spain



## 1. INTRODUCTION

Urolithiasis is a disease characterized by the presence of stones in the urinary tract, whether in the kidneys, ureters, or bladder. Its origin is multiple, and causes can be cited as hereditary, environmental, dietary, anatomical, metabolic, or infectious factors.<sup>1–3</sup> There are records that are more than 1000 years old related to urinary lithiasis. Hippocrates possessed an understanding about the disease and its characteristic symptoms in depth; there are even records of surgical procedures performed in antiquity.<sup>4</sup> The first study on the composition of a kidney stone was carried out around the year 1800 by Schellee and Bergman, chemicals and pharmaceuticals, who identified a uric acid stone.

A kidney stone (urolithiasis) is a biomaterial originating in the urinary tract following the principles of crystalline growth and, in most cases, cannot be eliminated naturally. This fact occurs mainly because the appropriate environment for the nucleation and subsequent formation of a germ is provided by crystal deposits around a crystalline nucleus and due to the difficulty in detecting their presence until there are clinical symptoms or they are large enough to be detected by imaging techniques.<sup>5</sup>

For the characterization of kidney stones, different analytical techniques have been employed, the pioneer among them being IR spectroscopy<sup>6</sup> and also Fourier transform infrared

spectroscopy (FT-IR)<sup>7,8</sup> that classify the results based on groups of compounds (uricite, oxalates, phosphates), and small crystalline or amorphous organic compounds have also been identified.<sup>9</sup> Of great importance are X-ray images;<sup>10–13</sup> techniques such as scanning electron microscopy (SEM) together with energy-dispersive X-ray spectroscopy (EDX) and thermogravimetry (TGA) help us understand the nature of kidney stones,<sup>14,15</sup> in addition to computed tomography (TC).<sup>15–17</sup>

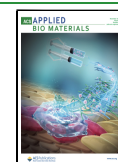
Physical techniques help in elemental analysis such as total reflection X-ray fluorescence (TXRF or TRXRF),<sup>18</sup> laser-induced decay spectroscopy (LIBS),<sup>19,20</sup> and inductively coupled plasma mass spectrometry by laser ablation (LA-ICP-MS) just to name a few. Thus, various chemical elements have been identified, with some belonging to phosphate class minerals and others falling into the organic class, such as oxalates, very frequently encountered in kidney stones.<sup>12</sup> Raman spectroscopy has also been applied, which allows the

**Received:** August 30, 2023

**Revised:** October 20, 2023

**Accepted:** October 23, 2023

**Published:** November 1, 2023



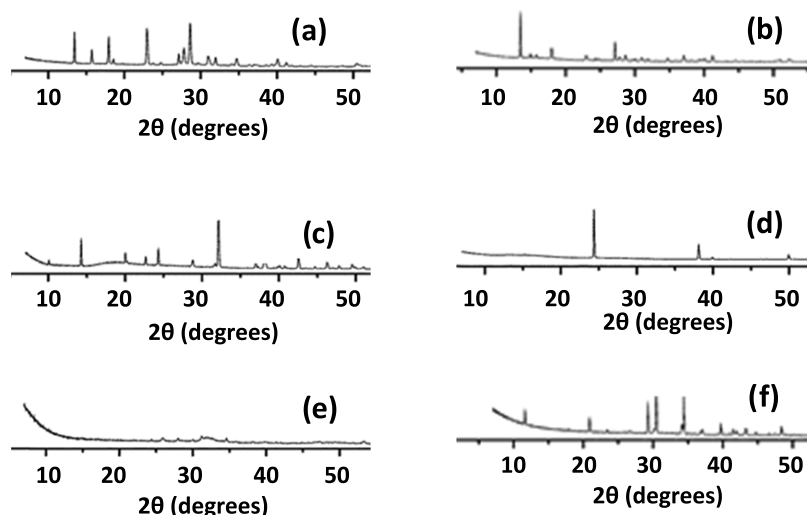


**Figure 1.** X-ray microdiffraction analyses: Badajoz Hospital: (a) uricite, (c) whewellite, and (e) calcium magnesium phosphate. Madrid Hospital: (b) uricite, (d) weddellite, (f) struvite.

identification of organic and inorganic compounds,<sup>21–23</sup> cathodoluminescence and thermoluminescence.<sup>24</sup> Biochemical methods have been the primary analytical techniques used to characterize the chemical composition of kidney stones.<sup>25,26</sup>

The main phases found in kidney stones are monohydrated and dihydrated oxalates, whewellite ( $\text{CaC}_2\text{O}_4 \cdot \text{H}_2\text{O}$ ) and weddellite ( $\text{CaC}_2\text{O}_4 \cdot 2\text{H}_2\text{O}$ ), respectively; phosphates such as brushite ( $\text{Ca}(\text{PO}_3\text{OH}) \cdot 2\text{H}_2\text{O}$ ), whitlockite ( $\text{Ca}_9\text{Mg}(\text{PO}_3\text{OH})_6(\text{PO}_4)_6$ ), struvite ( $\text{Mg}(\text{NH}_4)(\text{PO}_4) \cdot 6\text{H}_2\text{O}$ ), hydroxyapatite ( $\text{Ca}_5(\text{PO}_4)_3(\text{OH})$ ), and hydroxyapatite carbonates ( $\text{Ca}_5(\text{PO}_4)_x(\text{CO}_3)_{3-x}(\text{OH})$ ); and other compounds derived from uric acid, such as uricite, which is anhydrous uric acid ( $\text{C}_5\text{H}_4\text{N}_4\text{O}_3$ ), or dihydrate ( $\text{C}_5\text{H}_4\text{N}_4\text{O}_3 \cdot 2\text{H}_2\text{O}$ ) or ammonium urate ( $\text{NH}_4\text{C}_5\text{H}_3\text{N}_4\text{O}_3$ ).<sup>27</sup> Given such a variety of phases, mineral components are generally divided into three groups: oxalates, phosphates, and purines.

Worldwide, analyses related to the composition of kidney stones have been carried out in major regions: Europe,<sup>28,29</sup> Asia,<sup>30,31</sup> USA,<sup>32,33</sup> Mexico,<sup>34</sup> Africa,<sup>35–37</sup> and India.<sup>38</sup> The percentage incidence of renal lithiasis differs greatly in different parts of the world: in Asia it is 1–5%, in Europe it is 5–9%, in North America it is 13–15%, and in Saudi Arabia it is approximately 18–20%. In Spain, the prevalence rate is higher than 4% and, specifically, it rises to 14.3% in the Balearic Islands.

In Morocco, for example, according to some research, there are no up-to-date studies reporting the full prevalence of calcium oxalate throughout the country. However, there are only some statistics on calcium oxalate in some regions, especially in Rabat-Sale and Fez-Meknes with values of 66.6 and 60.98%, respectively.<sup>39</sup>

Kidney stones in which cystine appears ( $\text{SCH}_2\text{CH}(\text{NH}_2)\text{CO}_2\text{H}$ ) are rare. Cystine stones are produced by an inherited disorder of the transport of amino acid cystine that results in more than cystine in the urine.<sup>40</sup>

In this paper, 40 kidney stones are studied—22 of them were from the Don Benito, Badajoz University Hospital and 18 were from the Fundación Jiménez Daz (Madrid)—to establish differences between both populations with the same pathology and located in two very different regions in Spain.

## 2. MATERIALS AND METHODS

**2.1. Materials.** We analyzed 22 samples of kidney stones from the Don Benito Hospital of Badajoz with different shades, all of them with sequential crystalline growths whose original point is a crystallization nucleus and overlapping but perfectly identifiable layers. In general, the external zone of the kidney stones presents a reddish color and is less compact than the internal one. Don Benito is a municipality in the province of Badajoz, Spain, with a population of 37,310 inhabitants and a density of 66.42 inhabitants/km<sup>2</sup>; most of them reside in the urban center and work in the service sector, which, together with the food industry, comprise the main source of the city's vibrancy. The kidney stones were procured from the San Antonio hospital, a reference center for many inhabitants of the entire region belonging to different social statuses. However, the population can be considered to be of rural origin.

Madrid is the capital of Spain. It has a little more than three million registered inhabitants. The samples collected from the Fundación Jiménez Díaz University Hospital predominantly represent middle-class urban residents, totaling 18 samples with varying morphologies, compactness, and colors, although they mostly have reddish tones, with some exhibiting zoning. All kidney stones, extracted in both Don Benito (Badajoz) and Madrid, were obtained from surgical interventions in which the stones were removed.

**2.2. Methods.** Sample mineralogy was analyzed with powder X-ray microdiffraction (XRD) on a PAN Analytical X'Pert Pro X-ray diffractometer fitted with a Cu anode. The operating conditions were 40 mA, 45 kV, divergence slit of 0.5°, and 0.5 mm reception slits. The powder samples were scanned with a step size of 0.0167 (2θ) at 150 ms per step and 2θ angles of 5–60°. The detected phases were identified using the Crystallography Open Database (COD) library of crystal structures.

The microscopy and chemical analyses as well as the cathodoluminescence (CL) measurements were performed by scanning electron microscopy and energy-dispersive X-ray spectroscopy (SEM-EDS) using an Inspect-S ESEM instrument from the FEI Company.

Raman spectra of the samples were carried out by means of a Thermo-Fisher DXR Raman microscope (West Palm Beach, FL 33407) with a point-and-shoot Raman capability of 1 μm spatial resolution using a laser source at 532 nm.

CL spectra were prepared on polished slabs under a low vacuum mode without coating to maintain an open pathway for the CL emission, using a Gatan MonoCL3 detector with a PA-3 photomultiplier attached to the ESEM. The PMT covers a spectral range of 185–850 nm and is the most sensitive in the blue parts of the spectrum. A retractable parabolic diamond mirror and a photo-

multiplier tube are used to collect and amplify the luminescence signal. The sample was positioned ~10 mm beneath the bottom of the CL mirror assembly. The excitation for CL measurements was provided at a 20 kV electron beam.

### 3. RESULTS AND DISCUSSION

**3.1. By Powder X-ray Microdiffraction (XRD).** The analysis of X-ray microdiffraction on samples allowed the identification of major phases in the studied kidney stones, which are presented in Figure 1. The mineral phases that have been mostly identified in the samples from Madrid and Badajoz are listed in Table 1.

**Table 1. Abundance of Phases in the Studied Kidney Stones from Badajoz and Madrid Cities**

phases	Badajoz Hospital kidney stone (%)	Madrid Hospital kidney stone (%)
uricine	10	30
whewellite	50	40
wheddellite	15	5
cystine	0	5
phosphates	25	20

The most abundant phases in both populations are listed in Table 1. The predominant composition in both cities was whewellite, accounting for nearly 50%, with the notable absence of cystine and a scarcity of uric acid stones in the kidney stones from Badajoz. Phosphates were abundant in both locations, representing a quarter of the sample. In Madrid, calcium-based phosphates (apatite  $\text{Ca}_5(\text{PO}_4)_3(\text{OH})$  and brushite  $\text{CaHPO}_4 \cdot 2\text{H}_2\text{O}$ ), calcium–magnesium-based phosphates (whitlockite  $\text{Ca}_9\text{Mg}(\text{PO}_4)_6(\text{PO}_3\text{OH})$ ), and ammonium-based (struvite  $\text{NH}_4\text{MgPO}_4 \cdot 6\text{H}_2\text{O}$ ) stones were identified. Hydroxyfluorapatite, hydroxyapatite, and calcium–magnesium hydrogen apatite were found in kidney stones from Badajoz. The nonexistence of struvite in the studied Badajoz stones is striking. The presence of phosphates is conditioned by pH.<sup>41</sup> Struvite is a common compound that contributes significantly to water contamination in large cities.<sup>42,43</sup>

Uric acid and the corresponding urates act as essential biomineral phases in kidney stones, serving as crystalline seeds upon which different phases develop in successive crystallization stages.

Uric acid and its corresponding salts have been widely described<sup>39</sup> and constitute, in most kidney stones, the germ of the biomineral nucleation process. Uric acid is a biomineral that constitutes the main crystallization nuclei, generating

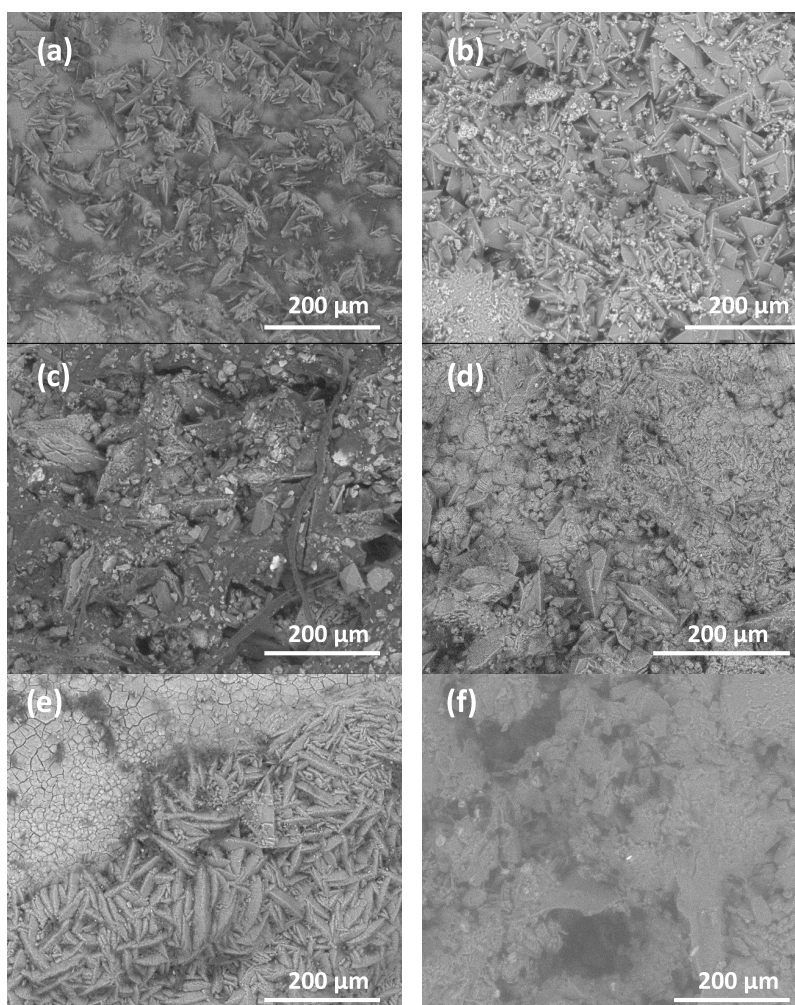


**Figure 2.** SEM-EDS analyses: Badajoz Hospital: (a) whewellite, (c) wheddellite and uricite, (e) left, phosphate; right, whewellite. Madrid Hospital: (b) whewellite, (d) uricite, and (f) phosphate.



epitaxial growths. Anhydrous uric acid or uricite<sup>8</sup> is the most thermodynamically stable form and is also the most frequent.

Oxalates, both monohydrate (whewellite) and dihydrate (weddelite), are very common biominerals that precipitate when urine is supersaturated with calcium, depositing on already crystallized materials such as urates and forming crystals with specific morphologies whose crystallization directs the urates into a heterogeneous nucleation process.<sup>37</sup> The two oxalates described, given the simple difference of presenting a varied number of water molecules, can undergo conversion by a reversible drying/hydration process, with the monohydrate being the most stable phase.<sup>44</sup> Lastly, cystine is a relatively uncommon phase that forms at acidic pH levels.<sup>45</sup>

### 3.2. By Scanning Electron Microscopy and Energy-Dispersive X-ray Spectroscopy (SEM-EDS) Analyses.

Figure 2 shows some of the images of the different kidney stones studied. Figure 2a,b shows images of calcium oxalate monohydrate (whewellite), which is usually present in most stones with its typical monoclinic prisms and clear exfoliation, indicating a higher pseudorhombic symmetry. The crystals are in a banded arrangement, suggesting a homogeneous nucleation due to the high supersaturation in the medium and which might be suspended when other substances with sizes less than the critical size appear in the system or due to competition in the available space to crystallize.

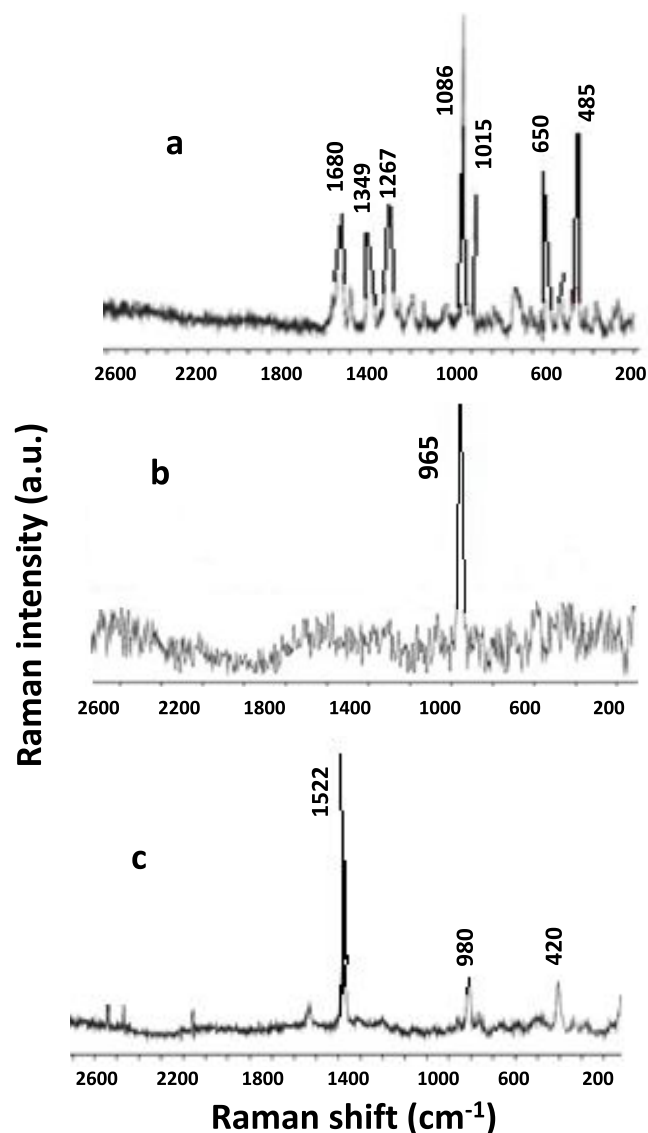
Figure 2c represents a kidney stone from Badajoz, and it presents a chaotic morphology corresponding to several crystalline phases that represent a heterogeneous nucleation based on oxalate. This type of nucleation is simpler than homogeneous nucleation since it only requires the presence of solid particles that can attract and retain on their surface the species that will constitute the eventual crystal. On the oxalate, in this case hydrated (weddelite, characterized by its tetragonal pyramids), uricite crystallizes together with organic matter. Once the nucleus is formed, subsequent crystal formation involves the combination of two processes: crystal growth and aggregation. Figure 2d shows the monoclinic prisms of the uricite, in this case, from a kidney stone in a Madrid Hospital; however, those identified from the Badajoz Hospital were also identical. Figure 2e displays the phosphatic formations (hexagonal morphology) present in the stones of the two cities, and in both cases, they participate in a heterogeneous nucleation with growth zonation. Phosphates are a group of biominerals typical of living organisms that can occur in various phases and with different cations, the most common being calcium, although magnesium or ammonium can also appear in their compositions. Figure 2e shows the phosphate phase with a hexagonal morphology in short prisms.

Figure 2f shows a struvite phosphate with a rhombic morphology. This phase is one of the most harmful in wastewater, and in large cities, it creates problems associated with its treatment and introduction into the circular economy.<sup>46–48</sup> The results obtained from the samples are in agreement with those obtained by X-ray microdiffraction analyses.

Cystine, an organosulfur amino acid compound with a hexagonal morphology and overlapping growths in layers and homogeneous nucleation, has been identified in a small sample of stones from Madrid. The crystals aggregate in a specific pattern, forming the characteristic morphology of cystine stones, which is rare in kidney stones.<sup>49</sup> The chemical composition of kidney stones has been found to be closely

related to various factors related to lifestyle, diet, and medication.

**3.3. By Raman Spectroscopy Analyses.** Raman spectroscopy was used to identify the mineral components of the kidney stones in this work (Figure 3). Three Raman spectra



**Figure 3.** Raman spectroscopy analyses: (a) uricite, (b) tricalcium phosphate, and (c) calcium oxalate hydrate.

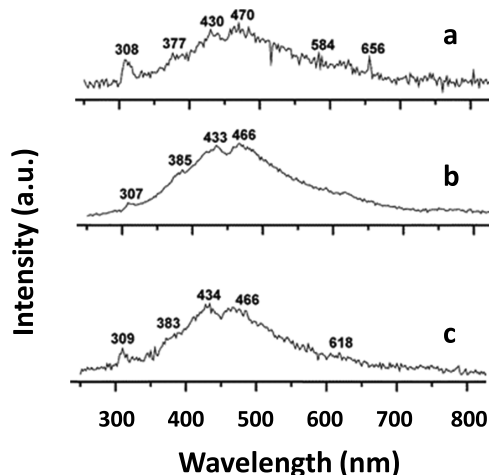
corresponding to samples rich in uricite, tricalcium phosphate, and calcium oxalate hydrate have been presented, which have been analyzed by comparison with similar standards.

Figure 3a presents typical Raman bands of uric acid, with three of moderate intensity: at 1685/1700  $\text{cm}^{-1}$  corresponding to the C=O stretching band of the carbonyl group, at 1580/1620  $\text{cm}^{-1}$  relative to the stretching band in the carbon–carbon bonds, and at 1330/1360  $\text{cm}^{-1}$  relative to the stretching of the carbon–nitrogen bond (C–N), and finally a band of weak intensity at 860/900  $\text{cm}^{-1}$  corresponding to the bending of the carbon–hydrogen bonds.<sup>50</sup> Figure 3b shows the Raman spectrum with typical bands of tricalcium phosphate with medium intensity at 420/450  $\text{cm}^{-1}$ , corresponding to Ca–O stretching; at 560/600  $\text{cm}^{-1}$  for the angular deformation of the phosphate group; and another at 1030/

1060  $\text{cm}^{-1}$  for the stretching of the P–O bond. In addition, the P–O stretching band is identified, which is the most intense in the spectrum at 940/970  $\text{cm}^{-1}$ .<sup>51</sup>

Finally, Figure 3c presents the Raman spectrum of calcium oxalate featuring the band at (a) 1480/1580  $\text{cm}^{-1}$  relative to the stretching of the C–C bonds of the oxalate anion having a high intensity; (b) 1320/1390  $\text{cm}^{-1}$  relative to the stretching vibration band of the carbonyl group (C=O) in the oxalate anion having a low intensity; (c) 750/800  $\text{cm}^{-1}$  relative to the C–O flexion band having a moderate intensity; and (d) 470/560  $\text{cm}^{-1}$  relative to the stretching of the calcium–oxygen (Ca–O) bonds in the crystalline calcium oxalate lattice having a medium intensity.<sup>52</sup>

**3.4. By Cathodoluminescence (CL) Analyses.** Figure 4 shows CL analyses of some of the phases present in the studied



**Figure 4.** CL analyses: (a) weddellite, (b)  $\text{CaMgHPO}_4$ , and (c) whewellite.

kidney stones corresponding to stones rich in weddellite, whitlockite, and whewellite. Each of the samples studied differs significantly in terms of both chemical and structural properties.

Weddellite and whewellite (Figure 4a,c) are two calcium oxalate minerals that frequently appear in kidney stones. Their crystal structures are similar; both have a monoclinic symmetry and a crystal lattice with alternating layers of calcium ions and oxalate molecules. However, there are differences in the arrangement of the oxalate ions in the two phases. Weddellite has a more ordered structure with oxalate ions arranged head-to-tail, while whewellite has a more disordered structure with oxalate ions arranged head-to-head and tail-to-tail. All this translates into different physical and chemical properties, such as solubility and reactivity and, of course, in the formation of kidney stones.<sup>53,54</sup>

Magnesium whitlockite (Figure 4b) and  $\beta$ -tricalcium phosphate are terms that are used interchangeably as it is difficult to distinguish the two phases by XRD analyses.<sup>55</sup> Magnesium whitlockite is found primarily in association with the pathologic mineralization of various soft tissues and stones. The characterization techniques capable of unequivocally distinguishing between different calcium phosphate phases are high-resolution imaging, crystallography, and/or spectroscopy as well as CL, which is a poorly crystalline apatite in which calcium ions are replaced by others existing in the human tract. Mg whitlockite is a pathological biomaterial.<sup>55</sup>

All of the CL spectra collected, although different, have low-intensity emission spectra with poorly defined bands related to the low crystallinity of the phases. The bands in the blue UV region from 200 to 480 nm are related to vacancies (intrinsic defects), linear or structural defects, and defects related to dehydroxylation, dehydration, or very frequent chemical reactions within the human body; in the 500/850 nm range, green infrared, it is related to extrinsic defects.

## 4. CONCLUSIONS

The description of the composition of kidney stones by means of different analytical techniques including XRD, SEM-EDS, Raman spectroscopy, and CL, collected from surgical interventions in two cities with very different lifestyles in Spain, Don Benito (Badajoz) and Madrid, can provide valuable information about the causes of the formation of kidney stones and try to generate protocols for their prevention.

The composition of the stones can lead to different treatments of the wastewaters of the two mentioned cities, which, of course, have different phases, especially in the wastewater treatment plants in relation to the presence of struvite in them. The variety of phases in kidney stones allows the identification of compounds, such as uricite, cystine, whitlockite, weddellite, whewellite, and struvite. SEM-EDS offers insights into the surface morphology and chemical composition, which are somewhat dispersed with infrequent but not significant chemical elements for their classification.

The techniques used in the analysis are complementary, and the less frequent Raman and CL techniques provide more precise information on the chemical and structural composition of kidney stones. These techniques can provide additional information about the crystallographic and molecular structures of the minerals present in the stones, identifying trace elements and impurities, and determining the chemical bonds and molecular structures of kidney stones. They are complementary techniques that explain more precise structural models.

CL provides information on the poor crystallinity of the phases and their hydration states (hydroxyl groups) as well as on the importance of bonds with the Ca cation in all structures. All of this is related to environmental and social factors of different population groups such as a high protein intake (see uricite), medications or bacterial factors (see struvite), and possible contamination with greenhouse gases (see cystine).

In general, the kidney stones procured from Badajoz Hospital are zonal stones, with the internal zone being clearer than the external one. In Madrid Hospital, there was a greater variety: they were zoned and had a single color. Regarding composition, the zonation in the stones responds to the same components; that is, the different states of crystallization are similar to varied aggregation situations that induce the crystallization of the same species.

The composition of kidney stones is very similar in both locations. The biggest difference is the presence of struvite in the calculi from Madrid. The nonexistence of struvite in kidney stones procured from the Badajoz Hospital means that this compound is barely detected in the sewage network of this city and lacks the environmental problems related to its elimination.

## AUTHOR INFORMATION

### Corresponding Author

Rosario García-Giménez – Departamento de Geología y Geoquímica, Facultad de Ciencias, Universidad Autónoma, 28049 Madrid, Spain; [orcid.org/0000-0002-7130-7945](https://orcid.org/0000-0002-7130-7945); Email: [rosario.garcia@uam.es](mailto:rosario.garcia@uam.es)

### Authors

Carmen González-Enguita – Hospital Universitario Fundación Jiménez Díaz, 28040 Madrid, Spain

Gonzalo Bueno-Serrano – Hospital Universitario Fundación Jiménez Díaz, 28040 Madrid, Spain

Andrés López de Alda-González – Hospital Don Benito, 06400 Don Benito, Badajoz, Spain

Complete contact information is available at: <https://pubs.acs.org/10.1021/acsabm.3c00722>

### Notes

The authors declare no competing financial interest.

## ACKNOWLEDGMENTS

The authors acknowledge Unidad de Litiasis, LEOC (Litotricia Extracorpórea por Ondas de Choque) and Endourología, Hospital Universitario Fundación Jiménez Díaz (HUFJD). Madrid, Spain. The authors are also thankful to Drs. J. Tabares Jiménez, M. Alcoba García, and D. Campos Valverde.

## REFERENCES

- Romero, V.; Akpinar, H.; Assimios, D. G. Kidney stones: a global picture of prevalence, incidence, and associated risk factor. *Rev. Urol.* **2010**, *12*, e86–e96.
- Vezzoli, G.; Dogliotti, E.; Terranegra, A.; Arcidiacono, T.; Macrina, L.; Tavecchia, M.; Pivari, F.; Mingione, A.; Brasacchio, C.; Nouvenne, A.; Meschi, T.; Cusi, D.; Spotti, D.; Montanari, E.; Soldati, L. Dietary style and acid load in an Italian population of calcium kidney stone formers. *Nutr. Metab. Cardiovasc. Dis.* **2015**, *25*, 588–593.
- Edvardsson, V. O.; Goldfarb, D. S.; Lieske, J. C.; Beara-Lasic, L.; Anglani, F.; Milliner, D. S.; Palsson, R. Hereditary causes of kidney stones and chronic kidney disease. *Pediatr. Nephrol.* **2013**, *28*, 1923–1942.
- López, M.; Hoppe, B. History, epidemiology and regional diversities of urolithiasis. *Pediatr. Nephrol.* **2010**, *25*, 49–59.
- Chatterjee, P.; Chakraborty, A.; Mukherjee, A. K. Phase composition and morphological characterization of human kidney stones using IR spectroscopy, scanning electron microscopy and X-ray Rietveld analysis. *Spectrochim. Acta, Part A* **2018**, *200*, 33–42.
- Beischer, D. E. Analysis of Renal Calculi by Infrared Spectroscopy. *J. Urol.* **1955**, *73* (4), 653–659.
- Estepa, L.; Daudon, M. Contribution of Fourier transform infrared spectroscopy. *Biospectroscopy* **1997**, *3*, 347–369.
- Khan, A. H.; Imran, S.; Talati, J.; Jafri, L. Fourier transform infrared spectroscopy for analysis of kidney stones. *Investig. Clin. Urol.* **2018**, *59* (1), 32–37.
- Cloutier, J.; Villa, L.; Traxer, O.; Daudon, M. Kidney stone analysis: “Give me your stone, I will tell you who you are!” *World J. Urol.* **2015**, *33*, 157–169.
- Haddad, M. C.; Sharif, H. S.; Shahed, M. S.; Mutaiery, M. A.; Samihan, A. M.; Sammak, B. M.; Southcombe, L. A.; Crawford, A. D. Renal colic: diagnosis and outcome. *Radiology* **1992**, *184* (1), 83–88.
- Sandhu, C.; Anson, K. M.; Patel, U. Urinary Tract Stones-Part I: Role of Radiological Imaging in Diagnosis and Treatment Planning. *Clin. Radiol.* **2003**, *58* (6), 415–421.
- Singh, V. K.; Rai, P. K. Kidney stone analysis techniques and the role of major and trace elements on their pathogenesis: a review. *Biophys. Rev.* **2014**, *6*, 291–310.
- Kahani, M.; Hariri Tabrizi, S.; Kamali-Asl, A.; Hashemi, S. A novel approach to classify urinary stones using dual-energy kidney, ureter and bladder (DEKUB) X-ray imaging. *Appl. Radiat. Isot.* **2020**, *164*, No. 109267.
- Lee, H. P.; Leong, D.; Heng, C. T. Characterization of kidney stones using thermogravimetric analysis with electron dispersive spectroscopy. *Urol. Res.* **2012**, *40* (3), 197–204.
- Manzoor, M. A. P.; Mujeeburahman, M.; Duwal, S. R.; Rekha, P. D. Investigation on growth and morphology of in vitro generated struvite crystals. *Biocatal. Agric. Biotechnol.* **2019**, *17*, 566–570.
- Federle, M. P.; McAninch, J.; Kaiser, J. A.; Goodman, P. C.; Roberts, C.; Mall, J. C. Computed tomography of urinary calculi. *Am. J. Roentgenol.* **1981**, *136*, 255–258.
- Odenrick, A.; Kartalis, N.; Voulgarakis, N.; Morsbach, F.; Loizou, L. The role of contrast enhanced computed tomography to detect renal stones. *Abdom. Radiol.* **2019**, *44*, 6542–6660.
- Kubala-Kukuś, A.; Arabski, M.; Stabrawa, I.; Banas, D.; Różanski, W.; Lipinski, M.; Majewska, U.; Wudarczyk-Mocko, J.; Braziewicz, J.; Pajek, M.; Gózd, S. Application of TXRF and XRPD techniques for analysis of elemental and chemical composition of human kidney stones. *X-Ray Spectrom.* **2017**, *46* (5), 412–420.
- Fang, X.; Ahmad, S. R.; Mayo, M.; Iqbal, S. Elemental analysis of urinary calculi by laser induced plasma spectroscopy. *Lasers Med. Sci.* **2005**, *20*, 132–137.
- Oztoprak, B. G.; González, J.; Yoo, J.; Gulecen, T.; Mutlu, N.; Russo, R. E.; Gundogdu, O.; Demire, A. Analysis and Classification of Heterogeneous Kidney Stones Using Laser-Induced Breakdown Spectroscopy (LIBS). *Appl. Spectrosc.* **2012**, *66* (11), 1353–1361.
- Mukherjee, A. K. Human kidney stone analysis using x-ray powder diffraction. *J. Indian Inst. Sci.* **2014**, *94*, 35–44.
- Tonannavar, J.; Deshpande, G.; Yenagi, J.; Patil, S. B.; Patil, N. A.; Mulimani, B. G. Identification of mineral compositions in some renal calculi by FT Raman and IR spectral analysis. *Spectrochim. Acta, Part A* **2016**, *154*, 20–26.
- Selvaraju, R.; Raja, A.; Thirupathi, G. FT-Raman spectral analysis of human urinary stones. *Spectrochim. Acta, Part A* **2012**, *99*, 205–210.
- Correcher, V.; Briatte, C.; Boronat, C.; García-Guinea, J. Radiation effect on cathodoluminescence and thermoluminescence emission of Ca-rich oxalates from the human body. *Luminescence* **2018**, *33*, 1438–1444.
- Uvarov, V.; Popov, I.; Shapur, N.; Abdin, T.; Gofrit, O. N.; Pode, D.; Duvdevani, M. X ray diffraction and SEM study of kidney stones in Israel: Quantitative analysis, crystallite size determination, and statistical characterization. *Environ. Geochem. Health* **2011**, *33* (6), 613–622.
- Oswald, I.; Cavalu, S.; Maghiar, T. T.; Osvat, D. Identification of Urinary Stone Composition upon Extracorporeal Shock Wave Lithotripsy. *Rom. J. Biophys.* **2011**, *21* (2), 107–112.
- Modlin, M.; Davies, P. J. The composition of renal stones analysed by infrared spectroscopy. *South Afr. Med. J.* **1981**, *59* (10), 337–341.
- González-Enguita, C.; García-Giménez, R.; García-Guinea, J.; Correcher, V. Spectral characterization of renal calculi collected from population in downtown Madrid (Spain). *Spectrochim. Acta, Part A* **2024**, *304*, No. 123395.
- Legay, C.; Haeusermann, T.; Pasquier, J.; Chatelan, A.; Fuster, D. G.; Dhayat, N.; Seeger, H.; Ritter, A.; Mohebbi, N.; Hernandez, T.; Stoermann Chopard, C.; Buchkremer, F.; Segerer, S.; Wuerzner, G.; Ammor, N.; Roth, B.; Wagner, C. A.; Bonny, O.; Bochud, M. Differences in the Food Consumption Between Kidney Stone Formers and Nonformers in the Swiss Kidney Stone Cohort. *J. Renal Nutr.* **2023**, *33* (4), 555–565.
- Guha, M.; Banerjee, H.; Mitra, P.; Das, M. The Demographic Diversity of Food Intake and Prevalence of Kidney Stone Diseases in the Indian Continent. *Foods* **2019**, *8*, 37–42.
- Deshpande, G.; Tonannavar, J.; Tonannavar, J.; Patil, S. B.; Kundargi, V. S.; Patil, S.; Mulimani, B. G.; Kalkura, S. N.; Ramya, J. R.; Arul, K. T. Detection of the mineral constituents in human renal



calculi by vibrational spectroscopic analysis combined with allied techniques Powder XRD, TGA, SEM, IR imaging and TXRF. *Spectrochim. Acta, Part A* **2022**, 270, No. 120867.

(32) Moe, O. W. Kidney calculi: pathophysiology and medical management. *Lancet* **2006**, 367, 333–344.

(33) Sunaryo, P. L.; May, P. C.; Holt, S. K.; Sorensen, M. D.; Sweet, R. M.; Harper, J. D. Ureteral Structures Following Ureterscopy for Kidney Stone Disease: A Population-based Assessment. *J. Urol.* **2022**, 208 (6), 1268–1275.

(34) Cruz-May, T. N.; Herrera, A.; Rodríguez-Hernández, J.; Basulto-Martínez, M.; Flores-Tapia, J. P.; Quintana, J. Structural and morphological characterization of kidney stones in patients from the Yucatan Maya population. *J. Mol. Struct.* **2021**, 1235 (5), No. 130267, DOI: 10.1016/j.molstruc.2021.130267.

(35) Bouatia, M.; Benramdane, L.; Idrissi, M. O. B.; Draoui, M. An epidemiological study on the composition of urinary stones in Morocco in relation to age and sex. *Afr. J. Urol.* **2015**, 21, 194–197, DOI: 10.1016/j.afju.2015.02.006.

(36) El Habbani, R.; Chaqroune, A.; Houssaini, T. S.; Arrayhani, M.; El Ammari, J.; Dami, F.; Chouhani, B. A.; Lahrichi, A. Étude épidémiologique sur les calculs urinaires dans la région de Fès et sur le risque de récurrence. *Prog. Urol.* **2016**, 26, 287–294.

(37) Mohim, M.; Kachkoul, R.; El Habbani, R.; Lahrichi, A.; Sqalli Houssaini, T. In vitro effect of Sidi Hrazem mineral water on the dissolution of calcium oxalate monohydrate calculi (Whewellite). *Sci. Afr.* **2022**, 16, No. e01187, DOI: 10.1016/j.sciaf.2022.e01187.

(38) Wilson, E. V.; Junaid Bushiri, M.; Vaidyan, V. K. Characterization and FTIR spectral studies of human urinary stones from Southern India. *Spectrochim. Acta, Part A* **2010**, 77 (2), 442–445.

(39) Abou-Elela, A. Epidemiology, pathophysiology, and management of uric acid urolithiasis: A narrative review. *J. Adv. Res.* **2017**, 8 (5), 513–527.

(40) Iordanidis, A.; García-Guinea, J.; Correcher, V.; Goundas, I. Optical and Spectral Observations on Cystine, Oxalate, and Apatite Renal Calculi. *Spectrosc. Lett.* **2011**, 44 (7–8), 490–494.

(41) Stefov, V.; Soptrajanov, B.; Kuzmanovski, I.; Lutz, H. D.; Engelen, B. Infrared and Raman spectra of magnesium ammonium phosphate hexahydrate (struvite) and its isomorphous analogues. III. Spectra of protiated and partially deuterated magnesium ammonium phosphate hexahydrate. *J. Mol. Struct.* **2005**, 752, 60–67.

(42) Leng, Y.; Soares, A. The mechanisms of struvite biomineralization in municipal waste water. *Sci. Total Environ.* **2021**, 799, No. 149261.

(43) Masindi, V.; Fosso-Kankeu, E.; Mamakoa, E.; Nkambule, T. T. I.; Mamba, B. B.; Naushad, M.; Pandey, S. Emerging remediation potentiality of struvite developed from municipal wastewater for the treatment of acid mine drainage. *Environ. Res.* **2022**, 210, No. 112944.

(44) Menon, M.; Mahle, C. J. Oxalate Metabolism and Renal Calculi. *J. Urol.* **1987**, 127, 148–151.

(45) Torricelli, F. C. M.; Scala Marchini, G.; De, S.; Yamaçake, K. G. R.; Mazzucchi, E.; Monga, M. Predicting Urinary Stone Composition Based on Single-energy Noncontrast Computed Tomography: The Challenge of Cystine. *Urology* **2014**, 83 (6), 1258–1264.

(46) Moulessehoul, A.; Gallart-Mateu, D.; Harrache, D.; Djaroud, S.; de la Guardia, M.; Kameche, M. Conductimetric study of struvite crystallization in water as a function of Ph. *J. Cryst. Growth* **2017**, 471, 42–52.

(47) Wei, S. P.; van Rossum, F.; van de Pol, G. J.; Winkler, M. K. H. Recovery of phosphorus and nitrogen from human urine by struvite precipitation, air stripping and acid scrubbing: A pilot study. *Chemosphere* **2018**, 212, 1030–1037.

(48) da Silveira Barcellos, D.; Procopiuck, M.; Bollmann, H. A. Management of pharmaceutical micropollutants discharged in urban waters: 30 years of systematic review looking at opportunities for developing countries. *Sci. Total Environ.* **2022**, 809, No. 151128, DOI: 10.1016/j.scitotenv.2021.151128.

(49) Guo, X.; Schmiede, P.; Assafa, T. E.; Wang, R.; Xu, Y.; Donnelly, L.; Fine, M.; Ni, X.; Jiang, J.; Millhauser, G.; Feng, L.; Li, X.

Structure and mechanism of human cystine exporter cystinosin. *Cell* **2022**, 185 (20), 3739–3752.

(50) Paluszkiwicz, C.; Kwiatek, W. M.; Zadło, A. Vibrational analysis of uric acid. *Spectrochim. Acta, Part A* **2004**, 60 (14), 215–220.

(51) Dubey, A. K.; Chakradhar, R. P. S.; Rao, J. L. Raman and infrared spectra of tricalcium phosphate (TCP) and hydroxyapatite (HAP) ceramics: vibrational analysis and density functional theory calculations. *J. Raman Spectrosc.* **2014**, 45 (2), 147–155.

(52) Li, Y.; Wei, L.; Hu, X.; Li, B.; Chen, J.; Zhou, X.; Zhang, Z. Label-free identification of calcium oxalate crystals in human urine using Raman spectroscopy. *BioMed Opt. Express* **2018**, 9 (3), 1153–1163.

(53) Hofbauer, J.; Steffan, I.; Höbarth, K.; Vujicic, G.; Schwetz, H.; Reich, G.; Zechner, O. Trace Elements and Urinary Stone Formation: New Aspects of the Pathological Mechanism of Urinary Stone Formation. *J. Urol.* **1991**, 145 (1), 93–96.

(54) Giannocari, M. G.; Marcelli, A.; Paoluzzo, L.; Ragni, R. Crystal structure of whewellite,  $\text{CaC}_2\text{O}_4 \cdot \text{H}_2\text{O}$ . *Am. Mineral.* **2000**, 85, 595–600.

(55) Shah, F. A. Magnesium whitlockite-omnipresent in pathological mineralisation of soft tissues but not a significant inorganic constituent of bone. *Acta Biomater.* **2021**, 125, 72–82.